

Manipulating $4f$ quadrupolar pair interactions in TbB_2C_2 using a magnetic field

A.M. Mulders¹, U. Staub¹, V. Scagnoli¹, Y. Tanaka², A. Kikkawa², K. Katsumata² and J.M. Tonnerre³

¹*Swiss Light Source, Paul Scherrer Institut, 5232 Villigen PSI, Switzerland*

²*RIKEN SPring-8 Center, Harima Institute, Sayo, Hyogo 679-5148, Japan and*

³*CNRS Grenoble, 38042 Grenoble Cedex 9, France*

(Dated: March 23, 2022)

Resonant soft x-ray Bragg diffraction at the $\text{Tb } M_{4,5}$ edges and non resonant Bragg diffraction have been used to investigate orbitals in TbB_2C_2 . The $\text{Tb } 4f$ quadrupole moments are ordered in zero field below T_N and show a ferroquadrupolar alignment dictated by the antiferromagnetic order. With increasing applied field along $[110]$ the $\text{Tb } 4f$ magnetic dipole moments rotate in a gradual manner toward the field. The quadrupole moment is rigidly coupled to the magnetic moment and follows this field-induced rotation. The quadrupolar pair interaction is found to depend on the specific orientation of the orbitals as predicted theoretically and can be manipulated with an applied magnetic field.

PACS numbers: 71.70.Ch; 75.40.Cx; 78.70.Ck

Correlation between conduction electrons and electronic orbitals leads to interesting materials properties such as metal-insulator transitions, colossal magneto resistance and superconductivity. Aspheric electronic orbitals, characterized by their quadrupole moment, may order and cause partial charge localization of the conduction electrons¹ or mediate coupling between cooper pairs.² Orbital order in f electron materials is dominated by coupling with the lattice (Jahn-Teller) or by indirect Coulomb interactions via the conduction electrons. That the latter can be important for intermetallic compounds was established theoretically^{3,4} but detailed experimental knowledge is limited due to the difficulty observing the associated orbital excitations. A recent neutron diffraction study provided evidence of a modulated quadrupolar motif in PrPb_3 , believed to be a direct consequence of indirect Coulomb interactions exhibiting oscillatory nature.⁵ The large orbital momentum of the f electronic shell also gives rise to a significant influence of higher multipole moments and may lead to hidden order phase transitions as demonstrated in the extensively studied URu_2Si_2 .⁶ Therefore it is important to understand the quadrupolar and higher order multipole pair interactions in these materials.

Quadrupolar order has been successfully investigated using neutron scattering in applied fields where induced magnetic moments reveal the underlying quadrupolar arrangement or motif. In addition, the relatively weak x-ray diffraction intensity of the quadrupole moments can be observed using synchrotron techniques allowing a *direct* determination of orbital motifs. Resonant x-ray scattering at the $L_{2,3}$ edge provided the first proof of the orbital motif in DyB_2C_2 .^{7,8} TbB_2C_2 is proposed to exhibit a transition from antiferromagnetic (AFM) to antiferroquadrupolar (AFQ) order in an applied magnetic field⁹ and is therefore an interesting candidate for investigation of its orbital interactions.

A magnetic field is time-odd and cannot couple to quadrupole moment which is time-even, but nevertheless in TbB_2C_2 the ordering temperature increases to

35 K, well above $T_N = 21.7$ K, in an applied magnetic field of 10 T. Consequently the interplay between dipole (time-odd) and quadrupole (time-even) moments can be readily investigated. Neutron diffraction studies revealed similarities between the magnetic structure in applied fields and the magnetic structure in the combined AFQ and AFM phase of DyB_2C_2 .¹⁰ However, resonant x-ray diffraction at the $\text{Tb } L_3$ edge suggests AFQ is present below T_N in zero field with a k vector component of $(0,0,\frac{1}{2})$ as found for DyB_2C_2 .¹¹

To test the suggested field-induced quadrupolar ordering we have investigated TbB_2C_2 in an applied magnetic field, H , with x-ray scattering techniques. We show that orbital order is present in the AFM phase of TbB_2C_2 at zero field, however, with ferroquadrupolar alignment which is dictated by the AFM structure. The quadrupoles are rigidly linked to the magnetic dipole moments and rotate with H along the $[110]$ direction. We show that, due to this rotation, the quadrupole pair interactions become stronger with applied field.

A single crystal of TbB_2C_2 was grown by Czochralski method using an arc-furnace with four electrodes. Samples were cut and polished perpendicular to the $[001]$ direction. The $(00\frac{1}{2})$ reflection was recorded at the $\text{Tb } M_{4,5}$ edges of TbB_2C_2 at the RESOXS end-station of the SIM beamline at the Swiss Light Source of the Paul Scherrer Institut. A permanent magnet provided a field of 1 T parallel to the $[110]$ direction in the scattering plane. In addition, non resonant x-ray Bragg diffraction of the $(01\frac{1}{2})$ and $(11\frac{1}{2})$ reflections was performed at the BL19LXU beam line at SPring-8 with 30 keV x-rays using a Ge solid-state detector to eliminate higher order harmonics. A cryomagnet provided H along the $[110]$ direction. In both sets of measurements, structure factors were derived from the integrated intensity, corrected for polarization, Lorenz factor, absorption and sample geometry.

The resonant Bragg diffraction results, Figure 1a, show the energy dependence of the $(00\frac{1}{2})$ reflection recorded at the $\text{Tb } M_{4,5}$ edges in zero field. The energy profile

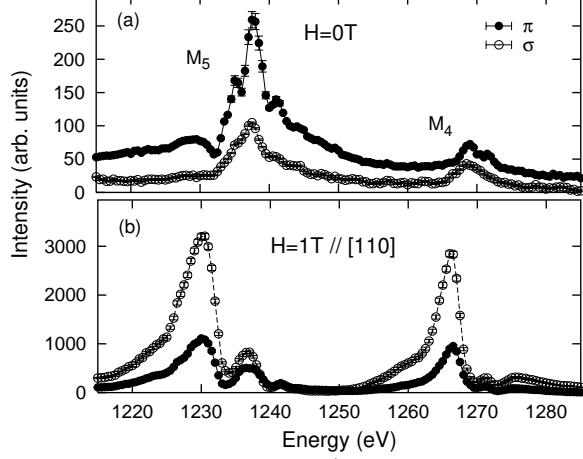


FIG. 1: Energy profile of the $(00\frac{1}{2})$ reflection at the Tb $M_{4,5}$ edges in TbB_2C_2 in (a) zero field and (b) applied field of 1 T along $[110]$, recorded with σ or π incident radiation at 11 K.

is independent of sample rotation about the Bragg wave vector. A significant part of the diffracted intensity is due to the total reflectivity of the polished sample. The $(00\frac{1}{2})$ diffracted intensity is relatively weak and appears magnetic in origin as witnessed by the relatively large intensity for incoming x-rays polarized in the scattering plane (π). In contrast, the diffracted intensity with $H = 1$ T, along the $[110]$ direction, shown in Fig. 1b is much stronger and strongest for incoming radiation polarized perpendicular to the scattering plane (σ). The energy profiles shown in Fig. 1 are expected to be insensitive to the magnetic structure, not to be confused with the total intensity that does depend on the magnetic structure. The drastic change with H indicates the presence of either an additional component of resonant scattering or a change in relative contribution of two different components of resonant scattering. The energy profile recorded in an applied magnetic field is similar to that recorded for the $(00\frac{1}{2})$ reflection in DyB_2C_2 in the AFQ phase.¹² This implies that for TbB_2C_2 , under the influence of an applied magnetic field of 1 T, the $(00\frac{1}{2})$ reflection is dominated by quadrupolar scattering.

The non resonant Bragg diffraction results illustrate that the quadrupole moment follows the magnetic moment rotation in applied fields. Fig. 2a,b shows the structure factors that relate directly to the order parameter, obtained from the integrated, non-resonant Bragg intensities of the $(01\frac{9}{2})$ and $(11\frac{15}{2})$ reflection as a function of applied field. In the AFM phase, at 15 K, the structure factors show a linear increase for applied fields below 1.5 T. In the paramagnetic phase, at 27 K, the ordered phase is entered above 3 T. The $(01\frac{9}{2})$ reflection appears at 3.2 T while the $(11\frac{15}{2})$ reflection appears at 3.5 T. However the evolution of the structure factor with increasing field is smooth for both reflections without a hint of a phase transition at 3.5 T for $(01\frac{9}{2})$. A similar behavior is observed as function of temperature in an applied field of 5 T (not shown). The intensities of $(01\frac{9}{2})$ and $(11\frac{15}{2})$ show a smooth decrease with increas-

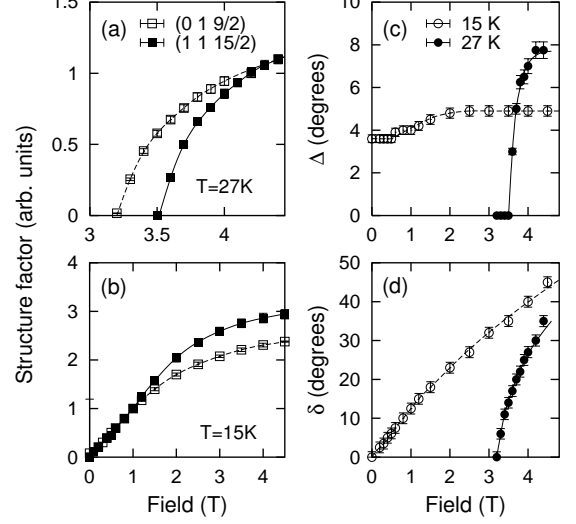


FIG. 2: Structure factor of the $(01\frac{9}{2})$ and $(11\frac{15}{2})$ reflection as function of applied magnetic field recorded with 30 keV at (a) $T = 27$ K and (b) $T = 15$ K. (c) and (d) show the deduced angles of Tb $4f$ orbital rotation as defined in Fig. 3.

ing temperature and disappear below 30 K and 29.5 K, respectively.

A structural transition with alternating displacements of the B and C atoms gives intensity in both type of reflections¹³ and cannot account for the present observation of intensity at $(01\frac{9}{2})$ and the absence of intensity at $(11\frac{15}{2})$. Magnetic, or time-odd, x-ray diffraction is generally weak and does not explain the magnitude of the observed intensity. We conclude that the scattering arises from time-even x-ray diffraction, i.e. from the aspheric charge distribution of the $4f$ shell, as such scattering can be intense.

To determine the structure factor it is assumed that the Tb ion on each site has the same charge distribution except for its specific orientation. Using the formalism for non resonant time-even scattering of Lovesey *et. al.*¹⁴ we deduce two independent Tb ions contribute and obtain for the structure factors:

$$F_{11\frac{1}{2}} \propto -2 [\sin(2\phi_1) - \sin(2\phi_3)] \langle Q_{11\frac{1}{2}} \rangle, \quad (1)$$

$$F_{01\frac{1}{2}} \propto [\cos(2\phi_1) - \cos(2\phi_3)] \langle Q_{01\frac{1}{2}} \rangle, \quad (2)$$

when the Miller index l equals an odd integer. The principal axis of the $4f$ orbital at atom n is canted in the ab -plane with respect to the $[100]$ direction with angle ϕ_n . $\langle Q_{hkl} \rangle$ is the expectation value of the Tb $4f$ time-even multipolar moment for a given field, temperature and Bragg wave vector $\mathbf{k} = (k_a, k_b, k_c)$:

$$\langle Q_{11\frac{1}{2}} \rangle \propto \frac{k_b^2}{k^2} \left[\langle j_2 \rangle \Psi_2^2 + 3\sqrt{3} \langle j_4 \rangle \Psi_2^4 - \sqrt{182} \langle j_6 \rangle \Psi_2^6 \right], \quad (3)$$

$$\langle Q_{01\frac{1}{2}} \rangle \propto \langle Q_{11\frac{1}{2}} \rangle + \frac{k_b^2}{k^2} \sqrt{21} \langle j_4 \rangle \Psi_4^4. \quad (4)$$

where Ψ_q^x is a structure factor of the chemical unit cell that is a linear sum of the atomic tensors, $\Psi_q^x = \langle T_q^x \rangle -$

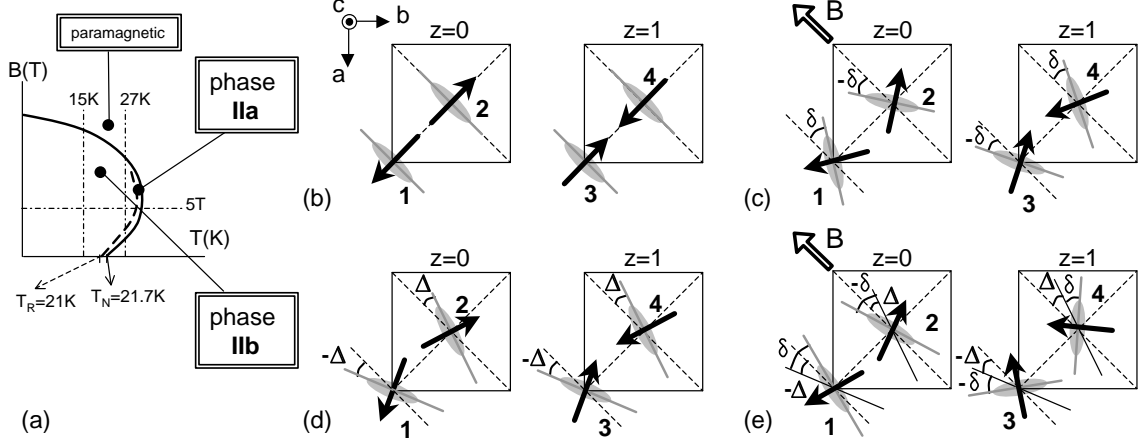


FIG. 3: (a) Phase diagram of TbB_2C_2 with magnetic field applied along $[110]$. (b) and (c) illustrate the orientation of magnetic moments (arrows) and quadrupole moments (ovals) in TbB_2C_2 in phase IIa in zero field and under applied fields, respectively. (d) and (e) illustrate phase IIb under the same conditions.

$\langle T_q^x \rangle$. $\langle T_q^x \rangle$ describes the asphericity of the Tb $4f$ electronic shell where $\langle T_2^2 \rangle$ equals the quadrupole moment, $\langle T_2^4 \rangle$ the hexadecapole moment and $\langle T_2^6 \rangle$ the hexacontatetrapole moment. $\langle j_2 \rangle$, $\langle j_4 \rangle$ and $\langle j_6 \rangle$ are Bessel function transforms of the radial distribution of the $4f$ electronic charge. In eqs. 3 and 4, $(k_c/k)^2 \sim 1$ and we neglect higher order terms $(k_b/k)^4$ and $(k_b/k)^6$ as $k_b/k \ll 1$.

We discuss the configuration of the quadrupoles but the order of the higher multipoles may alter also. When the $4f$ quadrupoles are aligned along $[110]$ ($\phi_1 = \phi_3 = \frac{3}{4}\pi$) as drawn in Fig. 3(b), $F_{01\frac{1}{2}}$ and $F_{11\frac{1}{2}}$ are both zero. When the $4f$ quadrupoles tilt toward the applied field with angle δ ($\phi_1 = \frac{3}{4}\pi + \delta$; $\phi_3 = \frac{3}{4}\pi - \delta$), Fig. 3(c), $F_{01\frac{1}{2}}$ is finite and $F_{11\frac{1}{2}}$ remains zero. Neutron diffraction shows that in the AFM phase the dipole moments tilt away from $\langle 110 \rangle$ with angle Δ , Fig. 3(d) ($\phi_1 = \frac{3}{4}\pi - \Delta$; $\phi_3 = \frac{3}{4}\pi + \Delta$).¹⁵ In this case, both $F_{01\frac{1}{2}}$ and $F_{11\frac{1}{2}}$ are zero in zero field while under an applied field both become finite (Fig. 3(e), $\phi_1 = \frac{3}{4}\pi - \Delta + \delta$; $\phi_3 = \frac{3}{4}\pi - \Delta - \delta$).

Consequently, at 27 K, between $H = 3.2$ and $H = 3.5$ T, the magnetic and quadrupolar structure of TbB_2C_2 is characterized by phase IIa. The quadrupoles are aligned parallel to $[110]$ as illustrated in Fig. 3(b) and are tilted in applied field as illustrated in Fig. 3(c). Above 3.5 T the compound is characterized by phase IIb. The quadrupoles are tilted away from the $[110]$ direction and neighboring atoms in the ab -plane are tilted in opposite directions as illustrated for $H = 0$ in Fig. 3(d) and for $H \neq 0$ in Fig. 3(e). We show the phase diagram schematically in Fig. 3(a) and define a reorientation temperature T_R by the boundary between phases IIa and IIb.

Multipole moment rotation in an applied field is linear for small δ , Δ (see Eq. (1)) hence the linear increase of the structure factor as observed at 15 K (see Fig. 2(b)). The magnetic moment of the $4f$ shell tilts toward the direction of the magnetic field and the time-even multipole moments follow accordingly, giving the observed contrast. This shows that (i) the coupling between magnetic and quadrupole moment is rigid and (ii) the orbitals

are already ordered in zero field, although with a ferro-quadrupolar alignment. This is consistent with the result in Fig. 1a as the ferroquadrupolar alignment in zero field does not contribute to scattering at $(00\frac{1}{2})$, whereas in an applied field, due to the orbital rotation, time-even scattering dominates (Fig. 1b).

The normalized structure factor of $(01\frac{1}{2})$ and $(11\frac{1}{2})$ reflections at 5 T with $9 \leq l \leq 17$ and are presented in Fig. 4. They are equal within the experimental uncertainty which shows that Ψ_4^4 is small (Eqs. 3 and 4). The solid line corresponds to Eqs. 1 and 3 with $\Psi_2^4/\Psi_2^2 = 0.5$ and $\Psi_2^6/\Psi_2^2 = 0.5$ and shows that the intensity can be attributed to time-even x-ray diffraction. The limited range of k makes the determination of Ψ_2^2 uncertain and this analysis merely confirms the absence of scattering from B and C atoms in contrast to DyB_2C_2 .¹³ Thus orbital order is present independent of a structural transition in TbB_2C_2 verifying the orbital interaction is mediated via the conduction electrons. A similar conclusion was reached for DyB_2C_2 from inelastic neutron scattering.¹⁶

With $\langle Q_{01\frac{1}{2}} \rangle = \langle Q_{11\frac{1}{2}} \rangle$ for a given field and temperature the angle Δ is deduced from the ratio between $F_{01\frac{1}{2}}$ and $F_{11\frac{1}{2}}$. In addition the quantity $\sin(2\delta)\langle Q_{hkl} \rangle$ follows from Eqs. 1 and 2 and δ has been estimated assuming $\langle Q_{hkl} \rangle$ is constant as a function of field and temperature. Both results are presented in Figs. 2(c) and (d). If $\langle Q_{hkl} \rangle$ increases with H the actual values for δ are lower than presented in Fig. 2d. Nevertheless, the increase in δ is gradual as a function of the applied field and reflects the orbital moment rotation.

The angle Δ is a result of the competition between the indirect Coulomb interaction and the magnetic exchange interaction between neighboring ions in the ab -plane. The first interaction favors perpendicular alignment of the quadrupoles while the latter favors a parallel alignment. An increase in Δ is observed with H . This shows that the relative strength of the indirect Coulomb interaction *increases* as the quadrupoles rotate perpendicular to each other in an applied field. To the authors

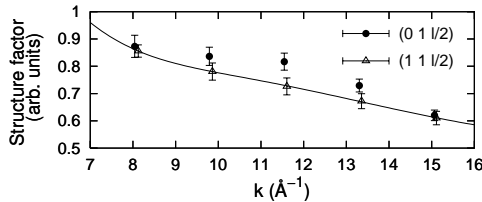


FIG. 4: Structure factor of $(01\frac{1}{2})$ and $(11\frac{1}{2})$ reflections at $B=5$ T and $T=2$ K. The solid line is a fit to Eq. 1.

knowledge, this is the first time that an increase in indirect Coulomb interaction has been observed in a straightforward manner. We also note that the determination of Δ is robust against changes in $\langle Q_{hkl} \rangle$ with applied field.

The increase in ordering temperature with applied field⁹ is in line with an antiferroquadrupolar interaction which becomes stronger when the angle between the orbitals moves from parallel to perpendicular alignment. The magnetic moments interact via the polarized spins of the conduction electrons while the multipolar moments interact via the charge density of the conduction electrons. In other words, charge screening by the conduction electrons changes when the $4f$ orbitals rotate and consequently the magnitude of the quadrupole pair interactions changes. This is consistent with the theoretical framework of Teitelbaum and Levy³ where electric multipole coupling via the conduction electrons depends on the relative angular positions of the ion cores.

The occurrence of combined AFQ and AFM below T_N is consistent with the quasi doublet ground-state.¹⁷ Re-

moval of the degeneracy of a doublet ground-state may account for one phase transition. Relaxation between the two singlets takes place above T_N and the magnetic and quadrupolar moments fluctuate. The increased energy separation between the two singlets below T_N is due to the magnetic exchange interaction, but both the magnetic and quadrupolar moment of the ground state singlet are observed, and this is illustrated by this study.

In conclusion, no magnetic field induced ordering of quadrupoles exists in TbB_2C_2 . The orbitals are already ordered in the AFM phase in zero field with a ferro-quadrupolar motif. On increasing the applied field along $[110]$ the Tb $4f$ magnetic moments rotate toward the field direction in a gradual manner. The quadrupole moment is rigidly coupled to the magnetic moment and follows this rotation. Neighboring Tb $4f$ orbitals move from parallel to perpendicular alignment and the quadrupolar pair interaction increases, witnessed by an increase of angle Δ between neighboring quadrupoles. This study shows that the quadrupolar pair interaction depends on the specific orientation of the orbitals as predicted for indirect Coulomb interaction via the conduction electrons and can be manipulated with an applied field.

We thank S.W. Lovesey for valuable discussion. This work was supported by the Swiss National Science Foundation and by a Grant-in-Aid for Scientific Research from the Japan Society for the Promotion of Science. This work was in part performed at the SLS of the Paul Scherrer Institute, Villigen PSI, Switzerland.

¹ S. Grenier, J. P. Hill, D. Gibbs, K. J. Thomas, M.v. Zimmermann, C. S. Nelson, V. Kiryukhin, Y. Tokura, Y. Tomioka, D. Casa, T. Gog, and C. Venkataraman, *Phys. Rev. B* **69**, 134419 (2004).

² T. Takimoto, *Phys. Rev. B* **62**, R14641 (2000).

³ H. H. Teitelbaum, and P. M. Levy, *Phys. Rev. B* **14**, 3058 (1976).

⁴ P. M. Levy, P. Morin, and D. Schmitt, *Phys. Rev. Lett.* **42**, 1417 (1979).

⁵ T. Onimaru, T. Sakakibara, N. Aso, H. Yoshizawa, H. S. Suzuki, and T. Takeuchi, *Phys. Rev. Lett.* **94**, 197201 (2005).

⁶ A. Kiss and P. Fazekas, *Phys. Rev. B* **71**, 054415 (2005).

⁷ Y. Tanaka, T. Inami, T. Nakamura, H. Yamauchi, H. Onodera, K. Ohoyama, and Y. Yamaguchi, *J. Phys.: Condens. Matter* **11**, L505 (1999).

⁸ K. Hirota, N. Oumi, T. Matsumura, H. Nakao, Y. Wakabayashi, Y. Murakami, and Y. Endoh, *Phys. Rev. Lett.* **84**, 2706 (2000).

⁹ K. Kaneko, H. Onodera, H. Yamauchi, T. Sakon, M. Motokawa, and Y. Yamaguchi, *Phys. Rev. B* **68**, 012401 (2003).

¹⁰ K. Kaneko, S. Katano, M. Matsuda, K. Ohoyama, H. Onodera, and Y. Yamaguchi, *Appl. Phys. A* **74**, S1749 (2002).

¹¹ D. Okuyama, T. Matsumura, H. Nakao, Y. Murakami, H. Onodera, A. Tobo, Y. Wakabayashi, and H. Sawa, *J. Phys. Soc. Jpn.* **74**, 1566 (2005).

¹² A. M. Mulders, U. Staub, V. Scagnoli, T. Nakamura, and A. Kikkawa, *Physica B* **378-380**, 367 (2006).

¹³ H. Adachi, H. Kawata, M. Mizumaki, T. Akao, M. Sato, N. Ikeda, Y. Tanaka, and H. Miwa, *Phys. Rev. Lett.* **89**, 206401 (2002).

¹⁴ S. W. Lovesey, E. Balcar, K. S. Knight, and J. Fernández-Rodríguez, *Phys. Rep.* **411**, 233 (2005).

¹⁵ K. Kaneko, H. Onodera, H. Yamauchi, K. Ohoyama, A. Tobo, and Y. Yamaguchi, *J. Phys. Soc. Jpn.* **70**, 3112 (2001).

¹⁶ U. Staub, A. M. Mulders, O. Zaharko, S. Janssen, T. Nakamura, and S. W. Lovesey, *Phys. Rev. Lett.* **94**, 036408 (2005).

¹⁷ M. Maino, A. Tobo, and H. Onodera, *J. Phys. Soc. Jpn.* **74**, 1838 (2005).